Trees, Forests and People 19 (2025) 100763

Contents lists available at ScienceDirect

Trees, Forests and People

journal homepage: www.sciencedirect.com/journal/trees-forests-and-people

Estimation of height and aerial biomass in *Eucalyptus globulus* plantations using UAV-LiDAR

Lucia Enriquez Pinedo [a,c], Kevin Ortega Quispe [a,c,*], Dennis Ccopi Trucios [a,c], Julio Urquizo Barrera [a], Claudia Rios Chavarría [a], Samuel Pizarro Carcausto [b], Diana Matos Calderon [c], Solanch Patricio Rosales [a], Mauro Rodríguez Cerrón [c], Zoila Ore Aquino [d], Michel Paz Monge [d], Italo Castañeda Tinco [a,c]

[a] *Dirección de Desarrollo Tecnológico Agrario, Instituto Nacional de Innovación Agraria (INIA), Carretera Saños Grande - Hualahoyo Km 8 Santa Ana, Junin 12006, Peru*

[b] *Centro de Investigación en Geomática Ambiental (CIGA), Instituto de Investigación para el Desarrollo Sustentable de Ceja de Selva (INDES-CES), Universidad Nacional Toribio Rodríguez de Mendoza, Chachapoyas 01001, Peru*

[c] *Facultad de Ciencias Forestales y del Ambiente, Universidad Nacional del Centro del Perú (UNCP), Av. Mariscal Castilla N° 3909, Junin 12006, Peru*

[d] *Dirección de Desarrollo Tecnológico Agrario, Instituto Nacional de Innovación Agraria (INIA), Av. La Molina 1981, Lima 15024, Peru*

ARTICLE INFO

Keywords:
Forest biomass
Remote sensors
LiDAR
Eucalyptus globulus
UAV

ABSTRACT

The lack of precise methods for estimating forest biomass results in both economic losses and incorrect decisions in the management of forest plantations. In response to this issue, this study evaluated the effectiveness of using the DJI Zenmuse L1 LiDAR, mounted on a DJI Matrice 300 RTK UAV, to provide three-dimensional measurements of canopy structure and estimate the aboveground biomass of Eucalyptus globulus. Various LiDAR metrics were employed alongside field measurements to calibrate predictive models using multiple regression and machine learning algorithms. The results at the individual tree level show that RF is the most accurate model, with a coefficient of determination (R^2) of 0.76 in the training set and 0.66 in the test set, outperforming Elastic Net (R^2 of 0.58 and 0.57, respectively). At the plot level, a multiple regression model achieved an R^2 of 0.647, highlighting LiDAR-derived metrics as key predictors. The findings revealed that the combination of LiDAR with advanced statistical techniques, such as multiple regression and Random Forest, significantly improves the accuracy of biomass estimation, surpassing traditional methods based on allometric equations. Therefore, the use of LiDAR in conjunction with machine learning represents an effective alternative for biomasss estimation, with great potential in such plantations and contribute to more sustainable exploitation of timber resources.

1. Introduction

A key global issue in the management of timber resources is the lack of precise and efficient methods for forest biomass estimation (Sa et al., 2024; Zhen et al., 2024). This deficiency not only limits the ability to assess the health of ecosystems and forests, but also carries significant economic implications. Accurate estimation of forest biomass is essential for the sustainable planning and management of timber resources, as it directly influences the economic valuation of forests and the efficient allocation of resources (Adhikari et al., 2024; Sillett et al., 2024; South et al., 2024). The lack of precise methods can lead to overestimation or underestimation of biomass, which affects the valuation of forest resources and, consequently, influences investment decisions and forestry exploitation policies (Konstantinavičienė, 2023). This inaccuracy causes considerable economic losses for forest owners and associated industries, while also limiting the ability to sustainably harness the economic potential of forest resources (Wu and Xu, 2023).

Eucalyptus globulus, commonly known as blue gum or Tasmanian blue gum, is a tree species native to Australia that has expanded globally due to its economic value and applications in the forest industry (Devi, 2023). This tree belongs to the Myrtaceae family and is characterized by its fast growth, high-quality wood, and aromatic properties (Mbula and Ngbolua, 2023) . Additionally, it is highly valued for its use in paper and pulp production, as well as in the essential oil industry due to the volatile compounds found in its leaves (Prajapati et al., 2024). However, in Peru, despite its commercial benefits, its expansion has raised concerns

* Corresponding author.
E-mail address: kevinorqu@gmail.com (K. Ortega Quispe).

https://doi.org/10.1016/j.tfp.2024.100763

Available online 22 December 2024

regarding its environmental impact (Panca et al., 2024). The introduction of this species into non-native ecosystems has posed challenges related to biodiversity and the alteration of local ecological cycles (Alonso and Castro, 2015). Therefore, while *Eucalyptus globulus* offers significant economic opportunities, its management must be carefully considered to minimize potential negative effects on Peruvian ecosystems, making the accurate estimation of its aboveground biomass a current necessity (Alrababah et al., 2009).

Aboveground biomass provides essential data on the amount of organic matter in trees, which is crucial not only for assessing forest productivity and health but also for the economic valuation of forest resources (Hirigoyen et al., 2021). This biomass includes branches, leaves, trunks, and other components, and is a key indicator of the economic value of timber resources (Y. Li et al., 2022). Understanding the quantity and distribution of this biomass enables an accurate assessment of the forest's economic potential, optimizing the planning of timber harvesting and the commercialization of forest products (Chen et al., 2018). Furthermore, accurate biomass estimation helps identify areas with high resource density that may be prioritized for economic investment and development, as well as for sustainable management (McRoberts et al., 2019).

Traditionally, the estimation of biomass has relied on the use of allometric equations and field methodologies. Although these methodologies are robust, they are highly labor-intensive and require considerable time and financial resources (Álvarez González et al., 2012; Corte et al., 2020; Schettini et al., 2022). These conventional methods often involve subjective visual measurements, such as estimating tree height, diameter at breast height (dbh), and crown diameter (Dantas et al., 2020; Malizia et al., 2020), which increases the likelihood of human error and reduces the accuracy of the calculations.

The incorporation of advanced technologies, such as LiDAR (Light Detection and Ranging), has revolutionized the way aboveground forest biomass estimation is conducted (Hall et al., 2005; Junttila et al., 2013; Lim et al., 2003; Torre-Tojal et al., 2022). In a LiDAR system, a sensor emits laser pulses that travel to the target and are reflected back to the sensor, where the time taken for the pulse to return allows for the exact calculation of the distance between the sensor and the target surface (Zhou and Li, 2023). This ability to obtain precise three-dimensional measurements enables the creation of detailed forest models, capturing data on tree height, canopy structure, and terrain topography with a level of detail that surpasses traditional methods (Almeida et al., 2021; da Cunha Neto et al., 2021; Jiang et al., 2022; Yin et al., 2024). This technology has proven to be particularly effective in large-scale studies, especially when used on airplanes and small aircraft, though the use of unmanned aerial vehicles (UAVs) offers additional advantages in local studies, improving the resolution and density of laser points (Potapov et al., 2021; Torresani et al., 2023).

The use of LiDAR in combination with UAVs represents a significant innovation in forest management (Corte et al., 2022; da Cunha Neto et al., 2021). LiDAR sensors mounted on these platforms not only provide precise and repeatable measurements but also offer a range of benefits that optimize forest management and promote sustainability (Scheeres et al., 2023; Tsouros et al., 2019). One of the main advantages of airborne LiDAR is its ability to capture detailed three-dimensional data of forest structure (Almeida et al., 2021; Fekry et al., 2022; Zhou and Li, 2023), including tree height (da Cunha Neto et al., 2021; Mielcarek et al., 2018; Yin et al., 2024), canopy density (Brede et al., 2022; De Luca et al., 2023; Hakkenberg et al., 2023), and terrain topography (da Silva et al., 2016). The use of UAVs equipped with LiDAR significantly reduces the need for extensive and laborious field campaigns, while enabling data capture over large and difficult-to-access areas more quickly and efficiently than traditional field sampling methods (Tamimi and Toth, 2024). This not only lowers the costs associated with fieldwork but also allows for the indirect estimation of tree height and the analysis of vertical forest structure, facilitating the development of highly accurate biomass prediction models (Duncanson et al., 2022; Li et al., 2023; Marcelo-Bazán et al., 2023).

To date, the application of LiDAR technology in forest biomass studies in Peru has not been reported, revealing a significant knowledge gap that needs to be addressed. To this end, the present study focused on estimating the average canopy height and aboveground biomass of *Eucalyptus globulus* plantations using UAV-mounted LiDAR, while also assessing the accuracy of this technology by determining the root mean square error (RMSE) of the deviations between the sensor data and the data obtained from field measurements. Additionally, this analysis seeks to validate the effectiveness of LiDAR under local conditions and explore its potential for future studies in forest ecosystems. This approach aims to provide a solid foundation for the application of LiDAR in forest resource management and assessment in Peru, promoting the adoption of advanced technologies to improve the accuracy and efficiency of forest biomass studies. Furthermore, the incorporation of this technology supports SDG 15: Life on Land, by providing more efficient tools for forest monitoring and management, promoting sustainable practices that protect biodiversity and reduce deforestation. On the other hand, it can also generate valuable data to support the implementation of more accurate forest policies, aligned with SDG 12: Responsible Consumption and Production, by optimizing the use of natural resources and minimizing environmental impacts (Tatay Nieto, 2020).

2. Materials and methods

2.1. Study site

The present study was conducted at "Fundo El Porvenir", located in the district of El Tambo, Junín Province, Peru. This area, situated in the Mantaro Valley, is characterized by *Eucalyptus globulus* plantations that began in the 1940s when the Cerro de Pasco Cooper Corporation acquired 150 hectares of land for forestry and livestock purposes. The original plantation was primarily intended for the production of structural timber for mining activities. During the military government, the property was nationalized and transferred to "Centromin Peru," and later, in 1992, it was handed over to the Peruvian Social Security Institute (ESSALUD). Currently, the area is used as a recreational zone for senior citizens, without active forest management (Arzapalo and Tinoco, 2023).

The topography of the estate (Fig. 1) is mostly flat with gentle undulations, and the altitude varies between 3600 and 3621 m. The climate is humid subtropical, with an average annual precipitation of 820 mm and temperatures ranging from 10 to 24 °C (Cáceres et al., 2024). The area is located at geodetic coordinates 75°14′5.99″ W and 12°2′13.20″ S. Despite the absence of recent forest management, a large portion of the plantation consists of stump sprouts, with trees of various age classes, reflecting natural growth after decades of limited forest exploitation.

This historical and ecological context provides a relevant scenario for this research, as the lack of forest management, natural regeneration, and variation in tree age allow for the study of biomass dynamics and other structural aspects of the forest.

2.2. Methodological framework

Fig. 2 presents the methodology used in the study, which will be detailed in the following sections. However, this sequential process begins with data collection, for which a UAV equipped with a LiDAR sensor was used to capture three-dimensional point clouds of the forest that represent its structure. Besides, field measurements were taken for parameters such as tree height (h) and diameter at breast height (dbh).

Subsequently, the process moved on to processing and modeling, where models of canopy height were generated from the LiDAR data and forest metrics were calculated. These metrics, along with the field data, were used to adjust predictive models that estimate biomass by plot and individual tree. To complete the process, an evaluation and validation of

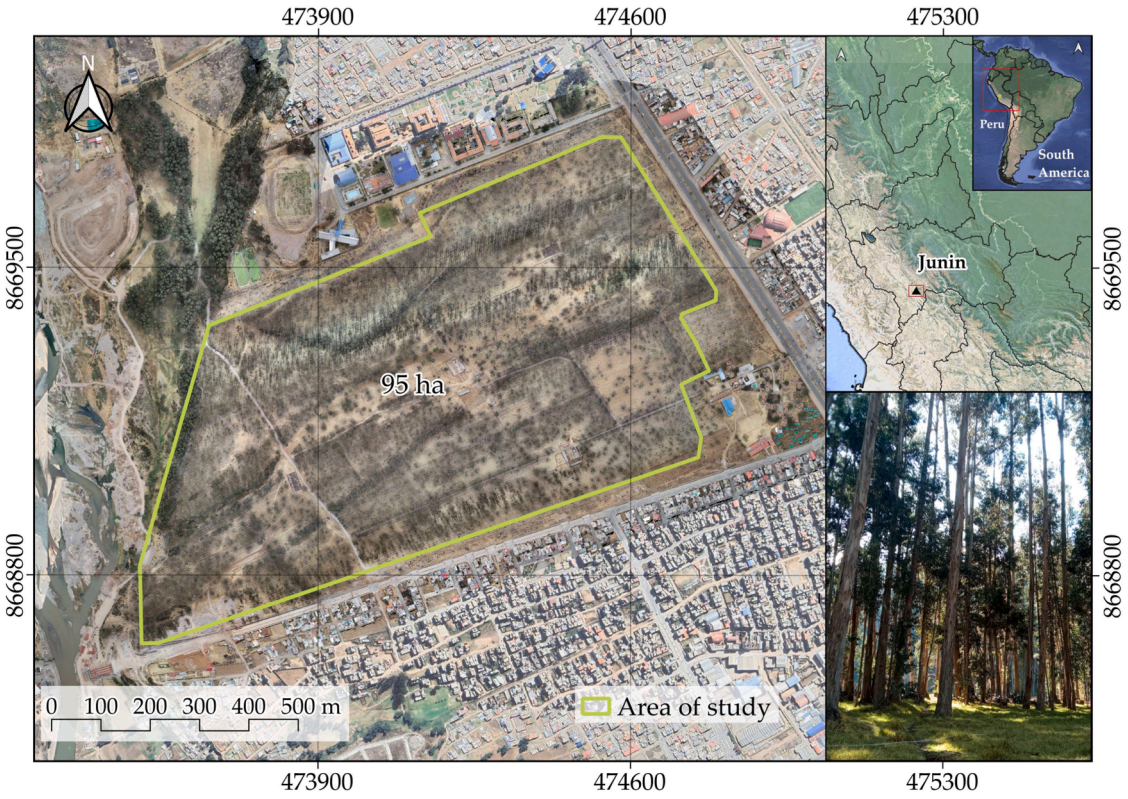

Fig. 1. Map of the study area.

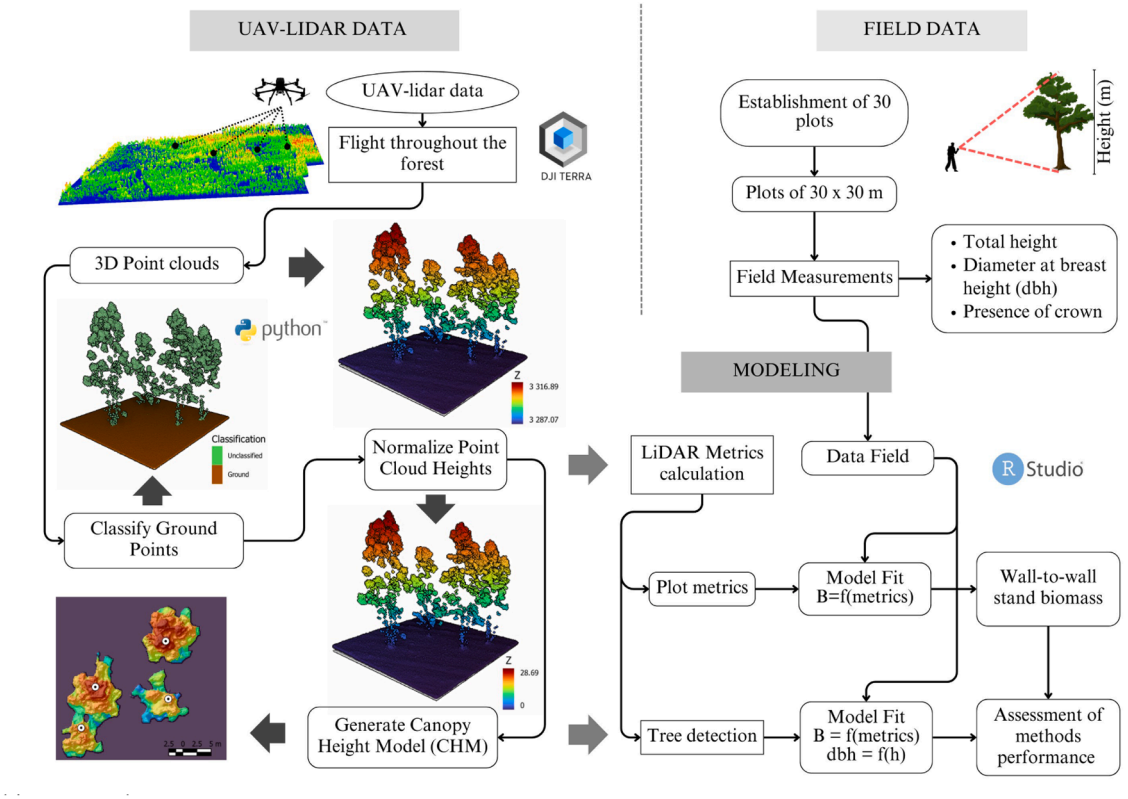

Fig. 2. The methodological approach of this study.

the results were conducted by comparing the estimates obtained through LiDAR with field measurements to ensure and improve the accuracy of the model.

The following schematic has been designed to provide a summary of all the procedures carried out in this ressearch.

2.3. Sampling design and field data collection

During the second half of 2023, a forest inventory was conducted, establishing 30 plots measuring 30×30 m (900 m²). These were distributed according to a systematic random sampling design based on stand density, which varied between areas of high and low tree density. Each of these plots was oriented in a north-south and east-west direction, and the coordinates of their four vertices were recorded using a high-precision RTK GNSS system. Within each plot, dendrometric variables were measured, such as tree height (h), diameter at breast height (dbh), and relative position. Each of the aforementioned processes are depicted in Fig. 3.

2.3.1. Tree position

The position of each tree (x, y) within the plot was recorded using the lower-left vertex (o) as the origin point and measuring the distances to the edges oriented to the north and east (Fig. 3). Subsequently, these relative coordinates were transformed into projected coordinates by adding the distances to the origin coordinates, allowing for an accurate representation of the location of each tree within the plot.

2.3.2. Dendrometric variables

Height estimation. The process of height estimation (h) in the field required the use of two tools: the hypsometer (Haglof Vertex Laser Geo, Långsele, Sweden), a sophisticated instrument designed to measure the height of trees and other objects, and the Trees v5.0 application (Forest Monitoring Tools, 2024), a service designed to estimate and monitor forest areas. The hypsometer, being part of the optical hypsometer family, uses principles of trigonometry and line of sight to indirectly determine height. The "Trees" application, on the other hand, allows for measurements to be taken directly in the field using the integrated sensors of a smartphone, eliminating the need to transport traditional equipment. Both tools utilize the clinometer method, measuring the angle of elevation and a known distance between the tree and the observer, facilitating the storage and analysis of large amounts of data. The formula used in the data extraction process is presented in Eq. (1), as established by López (2016).

$$Height = Distance\ x\tan\ (angle\ of\ elevation) \quad (1)$$

Estimation of diameter at breast height (dbh). The measurement of diameter at breast height (dbh) was performed using a measuring tape, following the standard methodologies described by Malleux (1970) for single-stem trees, measuring the diameter at 1.30 m height from the base. However, since the eucalyptus plantation features trees with multiple stems, the diameter was determined according to the methodology proposed by Cienciala et al. (2013), which is suitable for this type of tree structure. The equation representing the estimation of the equivalent dbh is shown in Eq. (2).

$$dbh = 2\sqrt{(DB_1/2)^2 + (DB_2/2)^2 + \ldots + (DB_n/2)^2} \quad (2)$$

Where, $DB_1, DB_2, \ldots, DB_n$ is the basal diameter of each stem (cm)

Calculation of aerial biomass. The estimation of aerial biomass per tree was performed using allometric formulas, which are based on mathematical relationships between tree size (diameter at breast height and total height). This allows for estimating the amount of biomass without the need to cut or damage the trees.

The diameter at breast height (dbh) and total height (h) data of the trees were obtained from the forest inventory conducted in the established plots during the pre-field stage. This data served as input for the equations used to estimate the weight of aerial biomass per tree, as shown in Eq. (3). This equation was extracted from Valverde et al. (2019), based on a study conducted under conditions similar to this research.

$$B_a = 90.45675 + 0.00071005 x dbh^2 x h^2 \quad (3)$$

Where B_a refers to the total aerial biomass in kg, (dbh) represents the diameter at breast height (cm), and (h) is the total height of the tree (cm).

Finally, the development of Eq. (4) was carried out, the result of which is the estimation of the total aerial biomass.

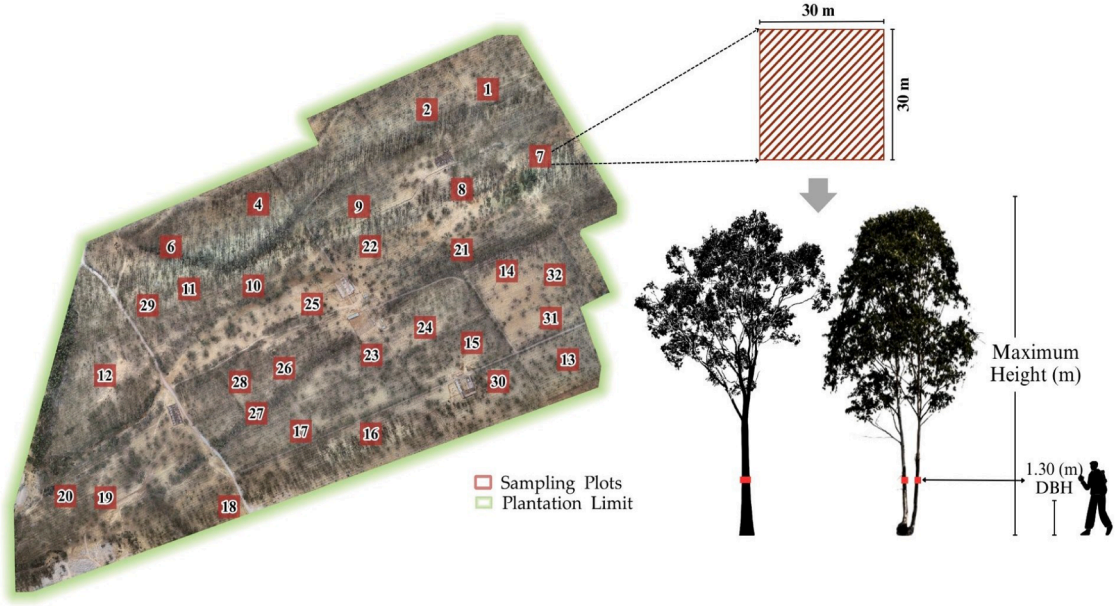

Fig. 3. Sampling design and field data collection.

$$B_{total} = \left(\frac{\sum AU}{1000}\right) x \left(\frac{10000}{Plot\ area}\right) \quad (4)$$

Where (B_{total}) represents the total aerial biomass (t/ha), and $(\sum AU)$ is the sum of the aerial biomass of all trees in the plot expressed in (kg/plot area).

2.4. UAV-LiDAR remote sensing data acquisition

The discrete return LiDAR data was acquired on August 21, 2023, using a DJI Zenmuse L1 sensor (DJI, Shenzhen, China), which integrates a Livox Lidar module (Livox Technology Company, Shenzhen, China) with a pulse frequency of 480 kHz for multiple returns (two returns), a high-precision inertial measurement unit (IMU), and an RGB camera, allowing for a planimetric accuracy of approximately 5 cm and a vertical accuracy of approximately 10 cm, with a scanning angle of 90° along the flight path. This sensor was mounted in a nadiral position on a 3-axis stabilized gimbal on the DJI Matrice 300 RTK UAV platform (Fig. 4).

The LiDAR data was collected during six flights that covered different parts of the study area. Each flight mission was designed using the Software DJI Pilot2 (DJI, Shenzhen, China), the interface of which is shown in Fig. 4. The flight path was organized in parallel lines, with a nominal height above the ground of 120 m, a speed of 10 m/s, and a 70 % overlap between flight lines, based on the sensor's swath width in relation to the scanning angle of the instrument, resulting in an average pulse density of 523 (ranging from 450 to 640 returns) per square meter.

2.5. Data processing and statistical analysis

2.5.1. Point cloud generation

To generate the point clouds, the software provided by the manufacturer DJI Terra (Beijing Green Valley Technology Co. Ltd., Beijing, China) was used, setting the following processing parameters: point cloud density at 100 % (all points), with the effective distance of the point cloud set at 250 m, coordinate system WGS 84/UTM Zone 18S + EGM2008, colored with true color from the RGB sensor and exported in LAS (binary format specified by the ASPRS) format, which is a widely used standard for storing and sharing data obtained through LiDAR technology. These unprocessed point clouds from each of the six flights were merged into a single point cloud and cropped to the study area; subsequently, duplicate points were removed using the software Cloud Compare (OpenGL, 2009).

2.5.2. Processing of the point cloud

Initially, we removed noise (very high or very low points) using the Statistical Outlier Removal (SOR) filtering algorithm, which first calculates the global mean distance along with the standard deviation of the distance from each point to each of its "k" nearest neighbors. Then, a threshold value is calculated by adding the global mean to the standard deviation multiplied by a predefined value, "m." We then iterate over each point and compare the mean distance with the calculated threshold; if it is greater than the threshold, it is marked as an outlier. The parameters k and m were set to 8 and 30, respectively, after testing different values and evaluating the results visually.

To produce the canopy height model (CHM), we performed ground filtering to label the returns as ground points and non-ground points using the Cloth Simulation Filter algorithm (Zhang et al., 2016) with default values for all parameters. We then normalized the point cloud, estimating the height above ground (HAG) of each point using the nearest classified ground points as a reference. Next, we applied the Pit-free algorithm (Khosravipour et al., 2014). With the generated CHM, we performed smoothing to reduce noise, employing a mean filter with a

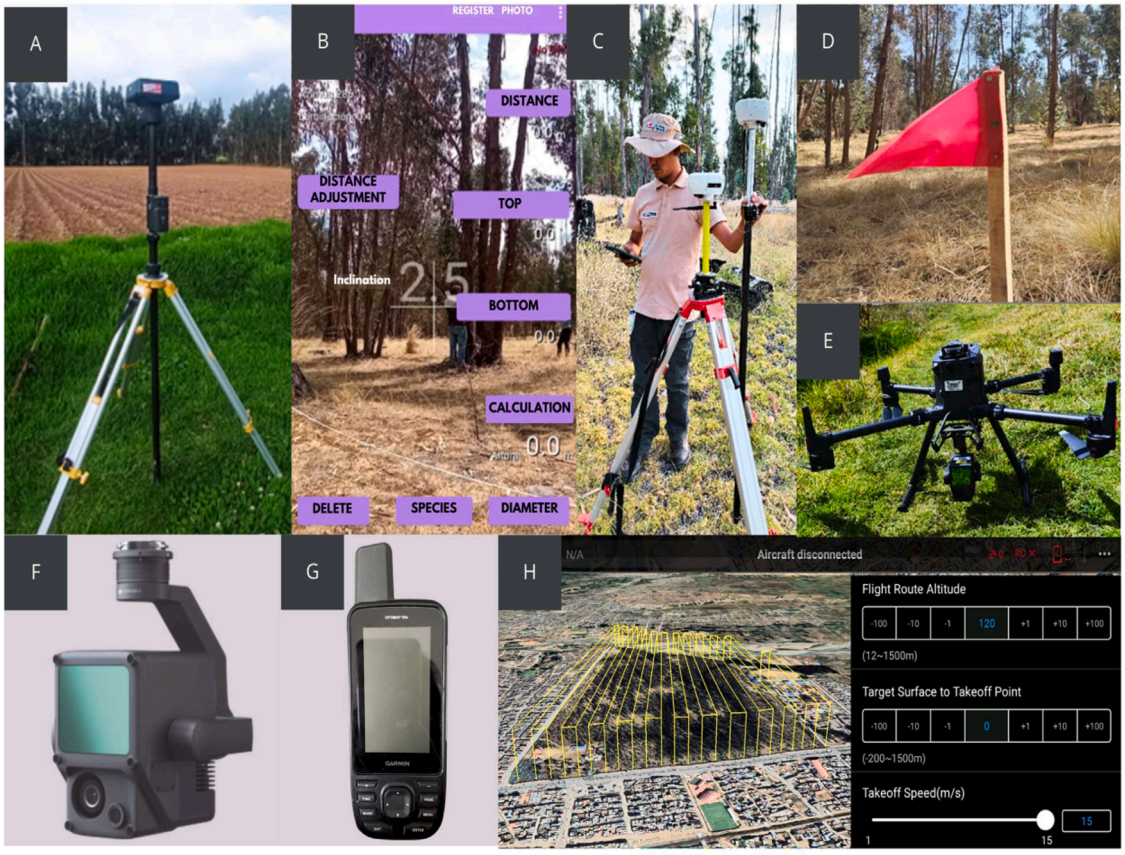

Fig. 4. (A) DJI RTK V2 GNSS, (B) Trees app, (C) GNSS receivers, (D) Control point - GPC, (E) Matrice 300 RTK, (F) DJI Zenmuse L1 (G) Global positioning equipment (H) Flight plan.

5 × 5 pixel window. Individual tree detection was done using the local maximum filter with a window of 6 × 6 m, which finds the highest value in reference to the tree canopies. These were converted into a vector point file. This process was carried out using the PDAL library (Butler et al., 2021) and SciPy (2024) in Python.

2.5.3. Extraction of metrics

To model biomass using the area-based approach (ABA), standard metrics were extracted from the normalized point cloud based on non-ground points, utilizing a vector polygon that defines the boundaries of the plots.

Similarly, for individual tree biomass modeling, the individual tree canopies were first segmented using the algorithm by Dalponte and Coomes (2016); this function uses the CHM and the tree locations, then applies the decision tree method to grow individual crowns around local maxima. The canopies were visually assessed in the GIS, and those with very irregular shapes were removed. The polygons of the canopies were used to extract standard metrics from the normalized point cloud using only non-ground points. This was accomplished using the LidR library (Roussel et al., 2020) in the R-project language.

2.6. Forest biomass estimation

2.6.1. Area-based approach (ABA) with statistical regression models

Multiple linear regression is a highly useful statistical tool in the forestry field, as it allows for understanding the relationship between independent variables, such as tree diameter and height, to predict biomass, which acts as the dependent variable (Zheng et al., 2022). This model is based on the assumption of a linear relationship between predictor variables and the response variable, making it crucial to verify assumptions such as normality, homoscedasticity, and the absence of multicollinearity to ensure reliable results (López-Serrano et al., 2019). Among the advantages of this model are its ability to quantify the individual contribution of each variable, provide confidence intervals for predictions, and facilitate the detection of outliers that could influence the overall fit and accuracy of the model (Zamudio et al., 2023). Furthermore, multiple linear regression can serve as a baseline model for comparison with more complex techniques, such as machine learning algorithms or nonlinear models, in the estimation of forest or agricultural biomass (López-Serrano et al., 2019; Zhang et al., 2020). Its simplicity and interpretability make it an effective method for performing quick estimates while also providing a direct understanding of the influence of biophysical variables on biomass accumulation.

To relate the standard metrics to the biomass values per plot, a correlation matrix was first created. Response variables were selected based on their low correlation with the dependent variable and the absence of high correlation with other variables. Then, different multiple linear regression models were fitted, evaluating the goodness of fit and the significance of the parameters. Using the best-fitting model, block-by-block predictions were made. Pixels where constructions were present were removed because they altered the metric values and overestimated the biomass.

2.6.2. Individual tree-based approach (ITD) with machine learning algorithms

The process of estimating individual tree biomass was carried out using machine learning with the Random Forest algorithm, a widely used machine learning technique in the forestry sector for biomass estimation (Zhu et al., 2020). This model builds multiple decision trees using the random sampling with replacement method (Bootstrapping) to extract a portion of the data as a training set and generate each regression tree (Wang et al., 2016). To estimate forest biomass, the algorithm combines the predictions of several decision trees and takes the average of these predictions as the final result (Li et al., 2022; Torre--Tojal et al., 2022). This ability to average multiple predictions reduces the risk of overfitting and improves accuracy.

On the other hand, the Elastic Net (ENET) algorithm is widely used in both agricultural and forestry fields, especially for its ability to handle multicollinearity and reduce overfitting. This model combines Ridge and LASSO regression techniques, allowing it to select the most significant variables and provide more robust predictions (Kc et al., 2024). The L1 and L2 regularization applied by ENET facilitates more accurate estimates in crop yield and forest biomass studies (Chen, 2024).

For training both algorithms, the dataset was split, assigning 70 % for training and 30 % for testing. For hyperparameter optimization in the regression models, cross-validation with grid search was used from the scikit-learn library (Pedregosa et al., 2012) in Python.

In the Random Forest model, three key hyperparameters were optimized: the number of trees, with values of 50, 100, 150, 200, and 250; the maximum number of features considered at each split (max_features), with values of 2 and 4; and the minimum number of samples required to split a node, ranging from 10 to 58 in increments of 4. For the Elastic Net model, two hyperparameters were optimized: L1_ratio, with values between 0.1, 0.2, 0.3, 0.4, 0.5, 0.6, 0.7, 0.8, 0.9, and alpha, with values of 0.01, 0.1, 1.0, 10.0, and 100.0. The objective of this methodology was to identify the combination of hyperparameters that would maximize the performance of the models evaluated using specific metrics.

3. Results

3.1. Coefficient of determination in estimating maximum height

The Fig. 5 shows a scatter plot comparing maximum heights recorded in the field with LiDAR-estimated data. The figure also shows a moderately strong positive relationship between the LiDAR measurements and the field measurements. This indicates that LiDAR can be a useful tool for estimating variables measured in the field, but it is important to note that it is not a perfect tool, and there are other sources of variability not captured by this model. $R^2 = 0.65$, meaning that 65 % of the variability in field measurements can be explained by the variability in LiDAR measurements. An R^2 of 0.65 suggests good accuracy in estimating field measurements using LiDAR data.

However, there is still 35 % of the variability that is not explained by the model. The difference between the measurements and the regression line represents the measurement error. This error may be due to several factors, such as instrument precision, weather conditions during measurement, or calibration errors in the equipment.

3.2. Correlation analysis between LiDAR metrics and biomass

Fig. 6a provides a clear representation of the relationships between variables such as *zsd, zmax, zmean*, and biomass at the plot level. To better understand these connections, detailed descriptions of these variables are available in the "supplementary materials" at the end of the document, as they are directly related to the structural characteristics of the eucalyptus plots. In this analysis, a complete correlation matrix was used to examine all available metrics and identify relevant patterns. From this matrix, the most influential variables for biomass estimation were identified as *zpcum1, zpcum5*, and *zentropy* due to their strong associations with biomass. In contrast, redundant or less relevant metrics were excluded. In the figure, larger and darker circles represent stronger correlations, with blue tones indicating positive relationships and red tones indicating negative ones. This visual representation simplifies the identification of key variables and their interactions, which are essential for understanding biomass dynamics at the plot level.

Meanwhile, Fig. 6b focuses on the correlations related to biomass estimation at the individual tree level. This analysis follows a similar approach to the plot-level analysis, presenting the relationships between predictor variables such as *zq15, zq95, zmax, zmean, zsd*, and *pzabovezmean*, along with the response variable, biomass. This allows for a deeper exploration of the connections between key variables, providing

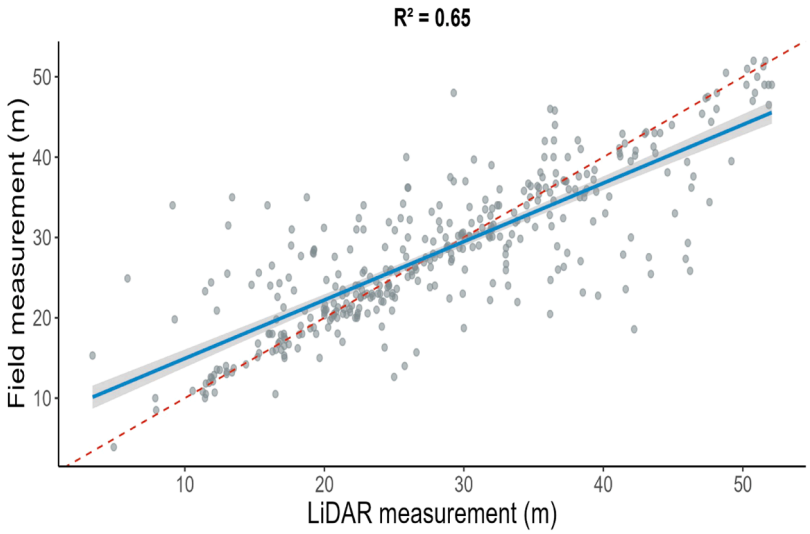

Fig. 5. Scatter plot of maximum heights measured in the field vs. estimated with LiDAR.

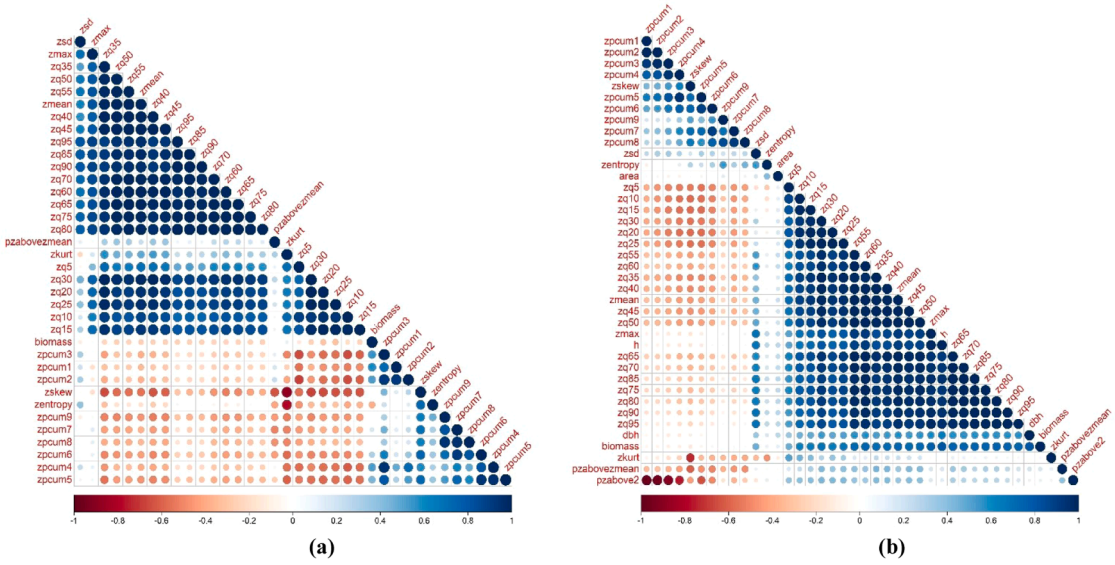

Fig. 6. a) correlation matrix between LiDAR metrics and biomass; b) correlation matrix between LiDAR metrics, height (h), diameter at breast height (dbh), biomass, and tree crown (area).

Table 1
Multiple linear regression model at the individual tree level, Random Forest (RF), Elastic Net (EN), Variables* = LiDAR metrics for forest structural analysis (supplementary material).

Metrics		Training	Test	Variables*	Hyper. RF		Hyper. Elastic Net	
RF	R^2	0.76	0.66	zq15				
	MRSE	0.77	0.91	zq95	Trees	50	L1_Ratio	0.60
	MAE	0.45	0.48	zmax	max_features	2	Alpha	1.00
EN	R^2	0.58	0.57	zmean	Nodes	14		
	MRSE	1.01	1.15	zsd				
	MAE	0.67	0.62	pzabovezmean				

insights into how they contribute to accurate biomass estimation at both individual tree and plot scales.

3.3. Estimation of biomass at the individual tree level

Table 1 compares the performance metrics of the models, Random Forest (RF) and Elastic Net (EN), in estimating the biomass of individual eucalyptus trees using variables obtained from the LiDAR sensor. For the RF model, the R^2 value is 0.76 in the training set and 0.66 in the test set, indicating strong a predictive power. The RMSE (root mean square error) is lower in training (0.77) compared to the test data (0.91), suggesting that the model makes minimal errors in estimating aerial biomass. The MAE (mean absolute error) values, which are 0.45 in training and 0.48 in testing, further reflect the consistent performance of

the model, with hyperparameters adjusted to 50 trees and 14 nodes per tree.

On the other hand, the Elastic Net model shows more modest performance, with an R^2 of 0.58 for training and 0.57 for testing, indicating limited predictive capacity. The RMSE is higher than that of the RF model, with 1.01 for training and 1.15 for testing, suggesting that the EN model tends to produce greater errors. Additionally, the MAE is 0.67 in training and 0.62 in testing, indicating that the errors are more pronounced compared to the RF model, with hyperparameters adjusted, such as an L1_Ratio of 0.60 and an Alpha of 1.00, reflecting the configuration of the Elastic Net model.

3.4. Estimation of maximum height at the individual tree level

For Random Forest (RF), Fig. 7 shows the training (A) and test (B) results in two scatter plots for maximum height. (A) corresponds to the training set, with a determination coefficient $R^2 = 0.76$, indicating that the model fits the data well and can accurately predict the biomass of eucalyptus during training. In graph (B), corresponding to the test set, $R^2 = 0.66$ suggests a decrease in estimation performance, although there is still a positive trend between the observed and predicted values. The blue line indicates the linear fit of the data, with a gray shadow representing the confidence interval.

Regarding Elastic Net (EN), the determination coefficients R^2 are 0.58 and 0.57, indicating a moderate fit in both training (A) and testing (B) respectively. The predicted values from the model also show a positive trend relative to the observed maximum height values, but with greater dispersion compared to the RF model. The blue regression line in both graphs has a gray shadow showing the confidence interval, and although there is a reasonable fit, the lower precision of the R^2 suggests that the Elastic Net model has more difficulty fully capturing the variability in the biomass data, especially at higher values.

3.5. Multiple linear regression model at the plot level

Table 2 highlights the key predictors for aerial biomass, revealing a

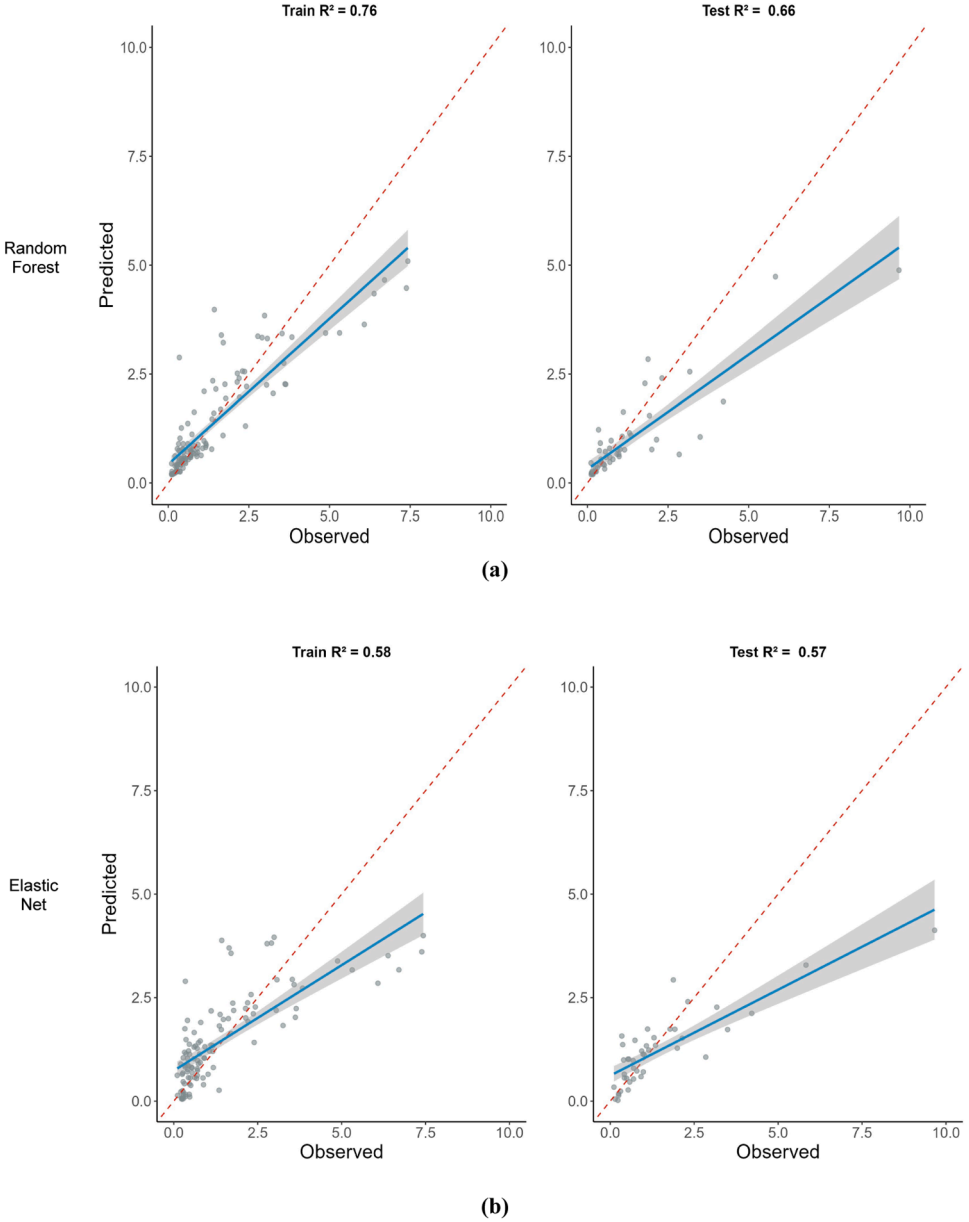

Fig. 7. Variable Maximum height; a) Training and testing of the predictive model generated by Random Forest; b) Training and testing of the predictive model generated by Elastic Net.

Table 2
Multiple linear regression model at the plot level.

Coefficients	Estimate	Std. Error	t value	Pr (>|t|)	Residual Standard error	Multiple R^2	Adjusted R^2	P-value
(Intercept)	2220.341	464.179	4.783	5.95e-05	134.1	0.684	0.647	1.118e-06
Zpcum1	19.549	5.494	3.558	0.00146				
Zpcum5	7.896	1.926	4.100	0.00036				
Zentropy	−2605.364	547.772	−4.756	6.39e-05				

robust and significant model that explains a substantial proportion of its variability. The coefficients were 19.549 (Zpcum1), 7.896 (Zpcum5), and −2605.364 (Zentropy), with p-values of 0.00146, 0.00036, and 6.39e-05, respectively, indicating their statistical significance. The model achieved an R^2 of 0.684, an adjusted R^2 of 0.647, and a residual standard error of 134.1.

These results demonstrate that Zpcum1 and Zpcum5 have positive impacts on aerial biomass, while Zentropy has a substantial negative effect. The sign of each coefficient reflects the direction of influence, with Zentropy suggesting that higher entropy is associated with reduced aerial biomass. Overall, the model effectively captures the relationships between these predictors and biomass variability.

The linear regression analysis for biomass estimation was conducted using three predictor variables: Zpcum1, Zpcum5, and Zentropy. The resulting predictive model is expressed in Eq. (5).

$$Biomass = 2220.34 + (19.549 \times zpcum1) + (7.896 \times zpcum5) - (2605.364 \times zentropy) \quad (5)$$

This equation indicates that for each unit increase in zpcum1, biomass increases by 19.549 units, while for each additional unit in zpcum5, biomass increases by 7.896 units. Additionally, an increase in zentropy reduces biomass by 2605.364 units. The intercept of 2220.341 represents the average biomass value when all predictor variables are zero. With an R^2 of 0.6471, this means that 64.71 % of the variability in biomass is explained by the variables zpcum1, zpcum5, and zentropy. Additionally, the global p-value (1.118e-06) confirms that the model is statistically significant. Each of the predictor variables is also significant ($p < 0.001$), suggesting that they have a considerable influence on biomass.

4. Discussion

Our study evaluated various LiDAR metrics, such as zpcum1, zpcum5, and zentropy, using multiple regression to predict aerial biomass in eucalyptus plantations. The results yielded a coefficient of determination (R^2) of 0.647, indicating a model with good predictive capacity and reduced errors. Furthermore, the p-value = 1.118e-06 confirms the statistical significance of the model. Previous studies have demonstrated the accuracy of remote sensing in estimating biomass in various forest plantations through advanced techniques, such as the use of UAVs and Structure from Motion (SfM). For instance, Estornell et al. (2024) reported an R^2 of 0.85 in orange plantations using SfM. Similarly, terrestrial laser scanning (TLS) achieved an R^2 of 0.966 when applying a coupled algorithm (Wang et al., 2024), highlighting the potential of these technologies in obtaining accurate biomass estimates, surpassing conventional methods.

However, other studies on different species, such as *Pinus radiata*, have reported an R^2 of 0.7 (Torre-Tojal et al., 2022), while the 3-PG model reached values between 0.78 and 0.88 (Bai et al., 2024). Furthermore, the extreme learning machine (ELM) technique, applied with ICESat-2 data, achieved an R^2 of 0.68 (Jiang et al., 2022), highlighting the importance of satellites for large-scale biomass estimation. These results demonstrate that the integration of remote sensing technologies with machine learning offers an opportunity to enhance the sustainable management of forest resources (Estornell et al., 2024; Wang et al., 2024).

On the other hand, our findings using LiDAR sensors and multiple regression yielded a coefficient of determination (R^2) of 0.647, indicating a moderately high predictive capacity for estimating aerial biomass across all plots. These results significantly improve the estimates obtained through the linear regression model ($R^2 = 0.34$) and even surpass models based on stereoscopic images and LiDAR sensors in other studies, where R^2 values were 0.42 (Liu et al., 2023). Compared to previous studies employing Synthetic Aperture Radar (SAR) data, which showed a non-linear relationship between biomass and height with errors of up to 10 % (Gama et al., 2010), our approach demonstrates a considerable reduction in the margin of error. Additionally, while allometric models applied in other contexts also resulted in statistically significant outcomes ($p < 0.01$) (Ounban et al., 2016), our p-value of 1.118e-06 robustly supports the statistical significance of the model, reinforcing the feasibility of using LiDAR for these estimates.

However, it is important to note that despite these advancements, limitations still persist, such as sensor dependency on specific environmental conditions and structural variability of eucalyptus in different regions. Moreover, future research could focus on integrating more ecological or climatic variables to further enhance predictive accuracy. Overall, these results highlight that remote sensing technologies, particularly through the use of LiDAR and advanced statistical approaches (Meunpong et al., 2024), provide an effective alternative to traditional methods for biomass estimation, offering greater accuracy and reducing the margin of error in commercial plantations.

The estimation of forest biomass, combining LiDAR data and remote sensing technologies such as multispectral and hyperspectral aerial photography, has proven to be highly effective. LiDAR captures the vertical structure of the forest, while aerial images provide a horizontal perspective, enhancing the accuracy of biomass models for species like eucalyptus (Gao et al., 2022). Machine learning methods, such as Random Forest (RF) and Neural Networks (NN), outperform traditional linear regression approaches, demonstrating better results when modeling biomass with high spatial resolution (Domingues et al., 2020; Santos et al., 2023).

However, although these approaches allow for detailed estimates, they still face challenges in terms of computational complexity and resource availability for large-scale implementation (Oehmcke et al., 2024; Ouattara et al., 2022). Studies utilizing LiDAR (Neuville et al., 2021; Spriggs et al., 2017; Van Aardt et al., 2008) indicate that, while there is some overestimation, the quantitative modeling of tree structure is a promising alternative for decision-making in forest management, providing a greater understanding of tree architecture and its biomass components.

This study employs LiDAR metrics to evaluate a 40-year-old *Eucalyptus globulus* plantation, addressing significant challenges related to its senescent condition and the difficult accessibility of the area. Unlike traditional methods, our approach is distinguished by its efficiency, significantly reducing the time and resources required, making it an innovative and practical alternative. To date, no studies have been reported in Peru or other Latin American countries that estimate the height and aboveground biomass of senescent plantations using drone-mounted LiDAR technology. Through this work, we aim not only to address this gap in the scientific literature but also to encourage the adoption of advanced technological tools to optimize the management of forest plantations, particularly in contexts where access and resources

are constrained.

5. Conclusions

Our findings demonstrate that the use of UAV-LiDAR combined with machine learning algorithms is proving to be an innovative and effective solution for forest management, particularly in estimating of maximum heights and aboveground biomass. This approach allows for an accurate three-dimensional representation of forest structure, capturing critical details such as tree height and canopy density, which are essential for efficient and sustainable forest management.

The LiDAR sensor mounted on UAVs shows significant advantages over traditional methods based on allometric equations and manual measurements, which are labor-intensive and prone to errors. Additionally, the LiDAR's ability to take precise measurements in hard-to-access areas expands the range of monitoring and assessment without the need for extensive field campaigns.

Random Forest (RF) demonstrated outstanding performance in predicting the maximum height of *Eucalyptus globulus*, outperforming the Elastic Net (EN) model in terms of accuracy. While RF achieved strong predictive capability in both training and test data, the EN model, though moderately accurate, showed greater dispersion in its prediction. In this sense, the RF model is more reliable for estimating the maximum height of *Eucalyptus globulus*.

When this technology is integrated with machine learning algorithms such as Random Forest, the accuracy of biomass prediction is improved, allowing the management of forest resources to be optimized.

The use of LiDAR data along with these algorithms allows for modeling biomass at a higher resolution and reducing the margin of error compared to conventional approaches. This is particularly relevant in commercial plantations, where resource optimization is key to efficient and sustainable timber exploitation.

Ethics statement

Not applicable: This manuscript does not include human or animal research.

Funding

This research was funded by the project "Creación del servicio de agricultura de precisión en los Departamentos de Lambayeque, Huancavelica, Ucayali y San Martín 4 Departamentos" CUI 2,449,640 del "Instituto Nacional de Innovación Agraria" (INIA) through the "Ministerio de Desarrollo Agrario y Riego (MIDAGRI)" of the Peruvian Government.

CRediT authorship contribution statement

Lucia Enriquez Pinedo: Writing – review & editing, Software, Methodology, Investigation, Formal analysis, Data curation. **Kevin Ortega Quispe:** Writing – review & editing, Writing – original draft, Validation, Formal analysis, Conceptualization. **Dennis Ccopi Trucios:** Writing – review & editing, Visualization, Software, Methodology, Investigation. **Julio Urquizo Barrera:** Writing – review & editing, Visualization, Methodology, Formal analysis. **Claudia Rios Chavarría:** Validation, Software, Methodology, Formal analysis, Data curation, Conceptualization. **Samuel Pizarro Carcausto:** Validation, Supervision, Software, Resources, Methodology, Investigation, Formal analysis, Data curation. **Diana Matos Calderon:** Validation, Supervision, Software, Resources, Methodology, Investigation, Funding acquisition. **Solanch Patricio Rosales:** Visualization, Validation, Software, Investigation, Formal analysis. **Mauro Rodríguez Cerrón:** Visualization, Validation, Supervision. **Zoila Ore Aquino:** Resources, Project administration, Funding acquisition. **Michel Paz Monge:** Resources, Project administration, Methodology, Funding acquisition. **Italo Castañeda Tinco:** Writing – original draft, Visualization, Validation, Software, Methodology, Investigation, Formal analysis.

Declaration of competing interest

The authors declare that they have no known competing financial interests or personal relationships that could have appeared to influence the work reported in this paper.

Acknowledgments

We would like to express our deepest gratitude to everyone who contributed to this research at the Santa Ana Experimental Station – Huancayo. Our thanks go to the volunteer students from the Faculty of Forestry and Environmental Sciences at the National University of Central Peru, the staff in charge of the "El Porvenir" farm, and especially to engineers Raúl Yaranga Cano and Walter Yaranga Cano for providing equipment, their valuable advice, and the facilities offered for access and management. We also extend our gratitude to Meliza Molina and Diego Fernández Ibarra for their knowledge and constant support both in the field and in the lab, and to Víctor Henry Pariona for his invaluable contribution to the topographic technical profile.

Supplementary materials

Supplementary material associated with this article can be found, in the online version, at doi:10.1016/j.tfp.2024.100763.

Data availability

Data will be made available on request.

References

Adhikari, D., Singh, P.P., Tiwary, R., Barik, S.K., 2024. Forest carbon stock-based bioeconomy: mixed models improve accuracy of tree biomass estimates. Biomass Bioenergy 183, 107142. https://doi.org/10.1016/J.BIOMBIOE.2024.107142.

Almeida, D.R.A.de, Broadbent, E.N., Ferreira, M.P., Meli, P., Zambrano, A.M.A., Gorgens, E.B., Resende, A.F., de Almeida, C.T., do Amaral, C.H., Corte, A.P.D., Silva, C.A., Romanelli, J.P., Prata, G.A., de Almeida Papa, D., Stark, S.C., Valbuena, R., Nelson, B.W., Guillemot, J., Féret, J.B., Chazdon, R., Brancalion, P.H. S., 2021. Monitoring restored tropical forest diversity and structure through UAV-borne hyperspectral and lidar fusion. Remote Sens. Environ. 264, 112582. https://doi.org/10.1016/J.RSE.2021.112582.

Alonso, A., Castro-Díez, P., 2015. Las invasiones biológicas y su impacto en los ecosistemas. Ecosistemas 24, 1–3. https://doi.org/10.7818/ECOS.2015.24-1.01.

Alrababah, M.A., Tadros, M.J., Samarah, N.H., Ghosheh, H., 2009. Allelopathic effects of Pinus halepensis and Quercus coccifera on the germination of Mediterranean crop seeds. New For (Dordr) 38, 261–272. https://doi.org/10.1007/S11056-009-9145-8/METRICS.

Álvarez González, J.G., Balboa Murias, M.Á., Merino García, A., Rodríguez Soalleiro, R., 2012. Estimación de la biomasa arbórea de "Eucalyptus globulus" y "Pinus pinaster" en Galicia. Recursos Rurais 1, 21–30.

Arzapalo, N., Tinoco, A., 2023. Percepción De La Arquitectura Accesible y El Nivel De Autonomía De Los Usuarios Del Centro del Adulto Mayor "El Porvenir" En Huancayo - 2023. Universidad Continental.

Bai, Y., Pang, Y., Kong, D., 2024. Integrating remote sensing and 3-PG model to simulate the biomass and carbon stock of Larix olgensis plantation. For Ecosyst 11, 100213. https://doi.org/10.1016/J.FECS.2024.100213.

Brede, B., Bartholomeus, H.M., Barbier, N., Pimont, F., Vincent, G., Herold, M., 2022. Peering through the thicket: effects of UAV LiDAR scanner settings and flight planning on canopy volume discovery. Int. J. Appl. Earth Obs. Geoinf. 114, 103056. https://doi.org/10.1016/J.JAG.2022.103056.

Butler, H., Chambers, B., Hartzell, P., Glennie, C., 2021. PDAL: an open source library for the processing and analysis of point clouds. Comput. Geosci. 148, 104680. https://doi.org/10.1016/J.CAGEO.2020.104680.

Cáceres, Y.Z., Torres, B.C., Archi, G.C., Mallqui, R.Z., Pinedo, L.E., Trucios, D.C., Quispe, K.O., 2024. Analysis of soil quality through aerial biomass contribution of three forest species in relict high andean forests of peru. Malaysian J. Soil Sci. 28, 38–52.

Chen, J., 2024. Linear regression analysis of the correlation between students' physical education performance and academic achievement in the context of smart physical education in colleges and universities. Appl. Math. Nonlin. Sci. 9. https://doi.org/10.2478/AMNS-2024-0641.

Chen, L., Ren, C., Zhang, B., Wang, Z., Xi, Y., 2018. Estimation of forest above-ground biomass by geographically weighted regression and machine learning with sentinel imagery. Forests 9, 1–20. https://doi.org/10.3390/f9100582.

Cienciala, E., Centeio, A., Blazek, P., Soares, Cruz Gomes, da, M., Russ, R., 2013. Estimation of stem and tree level biomass models for Prosopis juliflora/pallida applicable to multi-stemmed tree species. Trees - Struct. Funct. 27, 1061–1070. https://doi.org/10.1007/S00468-013-0857-1/METRICS.

Corte, A.P.D., de Vasconcellos, B.N., Rex, F.E., Sanquetta, C.R., Mohan, M., Silva, C.A., Klauberg, C., de Almeida, D.R.A., Zambrano, A.M.A., Trautenmüller, J.W., Leite, R. V., Do Amaral, C.H., Veras, H.F.P., Rocha, K., da, S., de Moraes, A., Karasinski, M.A., Sanquetta, M.N.I., Broadbent, E.N., 2022. Applying high-resolution UAV-LiDAR and quantitative structure modelling for estimating tree attributes in a crop-livestock-forest system. Land (Basel) 11. https://doi.org/10.3390/land11040507.

Corte, A.P.D., Rex, F.E., de Almeida, D.R.A., Sanquetta, C.R., Silva, C.A., Moura, M.M., Wilkinson, B., Zambrano, A.M.A., da Cunha Neto, E.M., Veras, H.F.P., de Moraes, A., Klauberg, C., Mohan, M., Cardil, A., Broadbent, E.N., 2020. Measuring individual tree diameter and height using gatoreye high-density UAV-lidar in an integrated crop-livestock-forest system. Remote Sens (Basel) 12. https://doi.org/10.3390/rs12050863.

da Cunha Neto, E.M., Rex, F.E., Veras, H.F.P., Moura, M.M., Sanquetta, C.R., Käfer, P.S., Sanquetta, M.N.I., Zambrano, A.M.A., Broadbent, E.N., Corte, A.P.D., 2021. Using high-density UAV-lidar for deriving tree height of araucaria angustifolia in an urban atlantic rain forest. Urban For Urban Green 63, 127197. https://doi.org/10.1016/J.UFUG.2021.127197.

da Silva, C.A., Duarte, C.R., Souto, M.V.S., dos Santos, A.L.S., Amaro, V.E., Bicho, C.P., Sabadia, J.A.B., 2016. Evaluating the accuracy in volume calculation in a pile of waste using UAV, GNSS and LiDAR. Boletim de Ciências Geodésicas 22, 73–94. https://doi.org/10.1590/S1982-21702016000100005.

Dalponte, M., Coomes, D.A., 2016. Tree-centric mapping of forest carbon density from airborne laser scanning and hyperspectral data. Methods Ecol. Evol. 7, 1236–1245. https://doi.org/10.1111/2041-210X.12575.

Dantas, D., Pinto, L.O.R., Terra, M., de, C.N.S., Calegario, N., de Oliveira, M.L.R., 2020. Reduction of sampling intensity in forest inventories to estimate the total height of eucalyptus trees. Bosque 41. https://doi.org/10.4067/S0717-92002020000300353.

De Luca, G., Praticò, S., Messina, G., Borgogno-Mondino, E., Modica, G., 2023. UAV LiDAR survey for forest structure metrics estimation in planning scenario. A Case Study on a Laricio Pine Forest in the Sila Mountains (Southern Italy). Lecture Notes in Computer Science (including subseries Lecture Notes in Artificial Intelligence and Lecture Notes in Bioinformatics) 14107 LNCS, 339–349. https://doi.org/10.1007/978-3-031-37114-1_23.

Devi, M., 2023. Eucalyptus : Why? Mahasweta Devi, pp. 164–167. https://doi.org/10.4324/9781003145363-24.

Domingues, G.F., Soares, V.P., Leite, H.G., Ferraz, A.S., Ribeiro, C.A.A.S., Lorenzon, A.S., Marcatti, G.E., Teixeira, T.R., de Castro, N.L.M., Mota, P.H.S., de Souza, G.S.A., de Menezes, S.J.M., da, C., dos Santos, A.R., do Amaral, C.H., 2020. Artificial neural networks on integrated multispectral and SAR data for high-performance prediction of eucalyptus biomass. Comput. Electron. Agric. 168, 105089. https://doi.org/10.1016/J.COMPAG.2019.105089.

Duncanson, L., Kellner, J.R., Armston, J., Dubayah, R., Minor, D.M., Hancock, S., Healey, S.P., Patterson, P.L., Saarela, S., Marselis, S., Silva, C.E., Bruening, J., Goetz, S.J., Tang, H., Hofton, M., Blair, B., Luthcke, S., Fatoyinbo, L., Abernethy, K., Alonso, A., Andersen, H.E., Aplin, P., Baker, T.R., Barbier, N., Bastin, J.F., Biber, P., Boeckx, P., Bogaert, J., Boschetti, L., Boucher, P.B., Boyd, D.S., Burslem, D.F.R.P., Calvo-Rodriguez, S., Chave, J., Chazdon, R.L., Clark, D.B., Clark, D.A., Cohen, W.B., Coomes, D.A., Corona, P., Cushman, K.C., Cutler, M.E.J., Dalling, J.W., Dalponte, M., Dash, J., de-Miguel, S., Deng, S., Ellis, P.W., Erasmus, B., Fekety, P.A., Fernandez-Landa, A., Ferraz, A., Fischer, R., Fisher, A.G., García-Abril, A., Gobakken, T., Hacker, J.M., Heurich, M., Hill, R.A., Hopkinson, C., Huang, H., Hubbell, S.P., Hudak, A.T., Huth, A., Imbach, B., Jeffery, K.J., Katoh, M., Kearsley, E., Kenfack, D., Kljun, N., Knapp, N., Král, K., Krůček, M., Labrière, N., Lewis, S.L., Longo, M., Lucas, R.M., Main, R., Manzanera, J.A., Martínez, R.V., Mathieu, R., Memiaghe, H., Meyer, V., Mendoza, A.M., Monerris, A., Montesano, P., Morsdorf, F., Næsset, E., Naidoo, L., Nilus, R., O'Brien, M., Orwig, D.A., Papathanassiou, K., Parker, G., Philipson, C., Phillips, O.L., Pisek, J., Poulsen, J.R., Pretzsch, H., Rüdiger, C., Saatchi, S., Sanchez-Azofeifa, A., Sanchez-Lopez, N., Scholes, R., Silva, C.A., Simard, M., Skidmore, A., Stereńczak, K., Tanase, M., Torresan, C., Valbuena, R., Verbeeck, H., Vrska, T., Wessels, K., White, J.C., White, L.J.T., Zahabu, E., Zgraggen, C., 2022. Aboveground biomass density models for NASA's Global Ecosystem Dynamics Investigation (GEDI) lidar mission. Remote Sens. Environ., 270 https://doi.org/10.1016/j.rse.2021.112845.

Estornell, J., Martí, J., Hadas, E., López-Cortés, I., Velázquez-Martí, B., Fernández-Sarría, A., 2024. Biomass estimation of abandoned orange trees using UAV-SFM 3D points. Int. J. Appl. Earth Obs. Geoinf. 130, 103931. https://doi.org/10.1016/J.JAG.2024.103931.

Fekry, R., Yao, W., Cao, L., Shen, X., 2022. Ground-based/UAV-LiDAR data fusion for quantitative structure modeling and tree parameter retrieval in subtropical planted forest. For Ecosyst 9, 100065. https://doi.org/10.1016/J.FECS.2022.100065.

Gama, F.F., dos Santos, J.R., Mura, J.C., 2010. Eucalyptus biomass and volume estimation using interferometric and polarimetric SAR Data. Remote Sens (Basel) 2, 939–956. https://doi.org/10.3390/rs2040939.

Gao, L., Chai, G., Zhang, X., 2022. Above-ground biomass estimation of plantation with different tree species using airborne LiDAR and hyperspectral data. Remote Sens (Basel) 14. https://doi.org/10.3390/rs14112568.

Hakkenberg, C.R., Tang, H., Burns, P., Goetz, S.J., 2023. Canopy structure from space using GEDI lidar. Front Ecol. Environ. 21, 55–56. https://doi.org/10.1002/FEE.2585.

Hall, S.A., Burke, I.C., Box, D.O., Kaufmann, M.R., Stoker, J.M., 2005. Estimating stand structure using discrete-return lidar: an example from low density, fire prone ponderosa pine forests. Forest Ecol. Manag. 208. https://doi.org/10.1016/j.foreco.2004.12.001.

Hirigoyen, A., Resquin, F., Navarro-Cerrillo, R., Franco, J., Rachid-Casnati, C., 2021. Stand biomass estimation methods for eucalyptus grandis and eucalyptus dunnii in Uruguay. Bosque 42, 53–66. https://doi.org/10.4067/S0717-92002021000100053.

Jiang, F., Sun, H., Ma, K., Fu, L., Tang, J., 2022. Improving aboveground biomass estimation of natural forests on the Tibetan Plateau using spaceborne LiDAR and machine learning algorithms. Ecol. Indic. 143, 109365. https://doi.org/10.1016/J.ECOLIND.2022.109365.

Junttila, V., Finley, A.O., Bradford, J.B., Kauranne, T., 2013. Strategies for minimizing sample size for use in airborne LiDAR-based forest inventory. Forest Ecol. Manag. 292. https://doi.org/10.1016/j.foreco.2012.12.019.

Kc, K., Romanko, M., Perrault, A., Khanal, S., 2024. On-farm cereal rye biomass estimation using machine learning on images from an unmanned aerial system. Precis Agric 1–28. https://doi.org/10.1007/S11119-024-10162-9/FIGURES/13.

Khosravipour, A., Skidmore, A.K., Isenburg, M., Wang, T., Hussin, Y.A., 2014. Generating pit-free canopy height models from airborne lidar. Photogramm Eng Remote Sens. 80, 863–872. https://doi.org/10.14358/PERS.80.9.863.

Konstantinavičienė, J., 2023. Assessment of potential of forest wood biomass in terms of sustainable development. Sustainability 15, 13871. https://doi.org/10.3390/SU151813871, 2023Page 13871 15.

Li, C., Yu, Z., Dai, H., Zhou, X., Zhou, M., 2023. Effect of sample size on the estimation of forest inventory attributes using airborne LiDAR data in large-scale subtropical areas. Ann. For. Sci. 80. https://doi.org/10.1186/s13595-023-01209-4.

Li, Y., Wang, R., Shi, W., Yu, Q., Li, X., Chen, X., 2022a. Research on accurate estimation method of eucalyptus biomass based on airborne LiDAR data and aerial images. Sustainability (Switzerland) 14. https://doi.org/10.3390/su141710576.

Li, Z., Bi, S., Hao, S., Cui, Y., 2022b. Aboveground biomass estimation in forests with random forest and Monte Carlo-based uncertainty analysis. Ecol. Indic. 142, 109246. https://doi.org/10.1016/J.ECOLIND.2022.109246.

Lim, K., Treitz, P., Wulder, M., St-Ongé, B., Flood, M., 2003. LiDAR remote sensing of forest structure. Prog. Phys. Geogr. 27, 88–106. https://doi.org/10.1191/0309133303pp360ra.

Liu, Y., Lei, P., You, Q., Tang, X., Lai, X., Chen, J., You, H., 2023. Individual tree aboveground biomass estimation based on UAV stereo images in a eucalyptus plantation. Forests 14. https://doi.org/10.3390/f14091748.

López, M.Á.L., 2016. Un procedimiento alternativo al tradicional para la medición de alturas con clinómetro. Madera y Bosques 11, 69–77. https://doi.org/10.21829/MYB.2005.1121257.

López-Serrano, P.M., Domínguez, J.L.C., Corral-Rivas, J.J., Jiménez, E., López-Sánchez, C.A., Vega-Nieva, D.J., 2019. Modeling of aboveground biomass with landsat 8 OLI and machine learning in temperate forests. Forests 11, 11. https://doi.org/10.3390/F11010011, 2020Page 11 11.

Malizia, A., Blundo, C., Carilla, J., Acosta, O.O., Cuesta, F., Duque, A., Aguirre, N., Aguirre, Z., Ataroff, M., Baez, S., Calderón-Loor, M., Cayola, L., Cayuela, L., Ceballos, S., Cedillo, H., Ríos, W.F., Feeley, K.J., Fuentes, A.F., Gámez Álvarez, L.E., Grau, R., Homeier, J., Jadan, O., Llambi, L.D., Rivera, M.I.L., Macía, M.J., Malhi, Y., Malizia, L., Peralvo, M., Pinto, E., Tello, S., Silman, M., Young, K.R., 2020. Elevation and latitude drives structure and tree species composition in Andean forests: results from a large-scale plot network. PLoS One 15, e0231553. https://doi.org/10.1371/JOURNAL.PONE.0231553.

Malleux, J., 1970. Estudio de la Relación D.A.P. con el diámetro de copa en un bosque húmedo sub tropical. Revista Forestal del Perú 4. https://doi.org/10.21704/RFP.V4I1-2.1089.

Marcelo-Bazán, F.E., Ila-Chavez, W.M., Baselly-Villanueva, J.R., Vargas-Aldave, J.C., Rajares-Callardo, U., 2023. Revista colombia forestal. Colombia forestal 26, 64–78. https://doi.org/10.14483/2256201X.19043.

Mbula, J.P., Ngbolua, K.-T.-N.J.-P., 2023. Etude Bibliographique sur la Phytochimie et les Activités Biologiques de Eucalyptus globulus L. (Myrtaceae). Revue Congolaise des Sci. Technol. 2, 220–232. https://doi.org/10.59228/RCST.023.V2.I1.28.

McRoberts, R.E., Næsset, E., Liknes, G.C., Chen, Q., Walters, B.F., Saatchi, S., Herold, M., 2019. Using a finer resolution biomass map to assess the accuracy of a regional, map-based estimate of forest biomass. Surv. Geophys. 40, 1001–1015. https://doi.org/10.1007/S10712-019-09507-1/METRICS.

Meunpong, P., Sangvisitpirom, P., Tangkit, K., Kaakkurivaara, N., Neimsuwan, T., Takuathung, C.N., Kaakkurivaara, T., Jenke, M., Jumwong, N., 2024. Biomass equations and annual growth of various Eucalyptus clones in commercial plantations across Thailand. Trees, Forests and People 17, 100647. https://doi.org/10.1016/J.TFP.2024.100647.

Mielcarek, M., Stereńczak, K., Khosravipour, A., 2018. Testing and evaluating different LiDAR-derived canopy height model generation methods for tree height estimation. Int. J. Appl. Earth Obs. Geoinf. 71, 132–143. https://doi.org/10.1016/J.JAG.2018.05.002.

Neuville, R., Bates, J.S., Jonard, F., 2021. Estimating forest structure from UAV-Mounted LiDAR point cloud using machine learning. Remote Sens (Basel) 13, 352. https://doi.org/10.3390/RS13030352, 2021Page 352 13.

Oehmcke, S., Li, L., Trepekli, K., Revenga, J.C., Nord-Larsen, T., Gieseke, F., Igel, C., 2024. Deep point cloud regression for above-ground forest biomass estimation from airborne LiDAR. Remote Sens. Environ. 302, 113968. https://doi.org/10.1016/J.RSE.2023.113968.

OpenGL, 2009. CloudCompare.

Ouattara, I., Korhonen, V., Visala, A., 2022. LiDAR-odometry based UAV pose estimation in young forest environment. IFAC-PapersOnLine 55, 95–100. https://doi.org/10.1016/J.IFACOL.2022.11.121.

Ounban, W., Puangchit, L., Diloksumpun, S., 2016. Development of general biomass allometric equations for Tectona grandis Linn.f. and Eucalyptus camaldulensis Dehnh. plantations in Thailand. Agric. Natural Resour. 50, 48–53. https://doi.org/10.1016/J.ANRES.2015.08.001.

Panca, M.P., Villanueva-Mamani, D.C., Gutierrez-Flores, I.R., 2024. Efecto alelopático de hojarascas de Eucalyptus globulus y Pinus halepensis en plantas silvestres Altoandinas, Perú: allelopathy in high Andean wild plants. Peru. Ecosistemas y Recursos Agropecuarios 11. https://doi.org/10.19136/ERA.A11N1.3505.

Pedregosa, F., Varoquaux, G., Gramfort, A., Michel, V., Thirion, B., Grisel, O., Blondel, M., Prettenhofer, P., Weiss, R., Dubourg, V., Vanderplas, J., Passos, A., Cournapeau, D., Brucher, M., Perrot, M., Duchesnay, É., 2012. Scikit-learn: machine Learning in Python. J. Mach. Learn Res. 12, 2825–2830.

Potapov, P., Li, X., Hernandez-Serna, A., Tyukavina, A., Hansen, M.C., Kommareddy, A., Pickens, A., Turubanova, S., Tang, H., Silva, C.E., Armston, J., Dubayah, R., Blair, J. B., Hofton, M., 2021. Mapping global forest canopy height through integration of GEDI and Landsat data. Remote Sens. Environ. 253. https://doi.org/10.1016/j.rse.2020.112165.

Prajapati, B., Sarvade, S., Prajapati, J., Shrivastava, A.K., Singh, M., 2024. Growing eucalypt outside its native range: a review on suitability and beneficial role. Int. J. Bio-resource and Stress Manag. 15, 01–12. https://doi.org/10.23910/1.2024.4981A.

Roussel, J.R., Auty, D., Coops, N.C., Tompalski, P., Goodbody, T.R.H., Meador, A.S., Bourdon, J.F., de Boissieu, F., Achim, A., 2020. lidR: an R package for analysis of Airborne Laser Scanning (ALS) data. Remote Sens. Environ. 251, 112061. https://doi.org/10.1016/J.RSE.2020.112061.

Sa, R., Nie, Y., Chumachenko, S., Fan, W., 2024. Biomass estimation and saturation value determination based on multi-source remote sensing data. Remote Sens (Basel) 16, 2250. https://doi.org/10.3390/RS16122250/S1.

Santos, J.S., Mendonça, A.R.de, Gonçalves, F.G., Silva, G.F.da, Almeida, A.Q.de, Carvalho, S.de P.C.e., Silva, J.P.M., Carvalho, R.C., Silva, E.F.da, Aguiar, M.O., 2023. Predicting eucalyptus plantation growth and yield using Landsat imagery in Minas Gerais. Brazil. Ecol Inform 75, 102120. https://doi.org/10.1016/J.ECOINF.2023.102120.

Scheeres, J., de Jong, J., Brede, B., Brancalion, P.H.S., Broadbent, E.N., Zambrano, A.M. A., Gorgens, E.B., Silva, C.A., Valbuena, R., Molin, P., Stark, S., Rodrigues, R.R., Santoro, G.B., Resende, A.F., de Almeida, C.T., de Almeida, D.R.A., 2023. Distinguishing forest types in restored tropical landscapes with UAV-borne LIDAR. Remote Sens. Environ. 290, 113533. https://doi.org/10.1016/J.RSE.2023.113533.

Schettini, B.L.S., Jacovine, L.A.G., Torres, C.M.M.E., Carneiro, A., de, C.O., Castro, R.V. O., Villanova, P.H., da Rocha, S.J.S.S., Rufino, M.P.M.X., Neto, S.N., de, O., Júnior, V.T.M., de, M., 2022. Use of destructive and non-destructive methodologies to estimate stem biomass accumulation and carbon stock in an eucalyptus forest. Revista Arvore 46, 1–9. https://doi.org/10.1590/1806-908820220000011.

SciPy, 2024. SciPy. URL https://scipy.org/(accessed 10.5.24).

Sillett, S.C., Graham, M.E., Montague, J.P., Antoine, M.E., Koch, G.W., 2024. Ground-based calibration for remote sensing of biomass in the tallest forests. Forest Ecol. Manag. 561, 121879. https://doi.org/10.1016/J.FORECO.2024.121879.

South, P.B.M., Finley, A.O., Lansing, E., 2024. Calibrating satellite maps with field data for improved predictions of forest biomass.

Spriggs, R.A., Coomes, D.A., Jones, T.A., Caspersen, J.P., Vanderwel, M.C., 2017. An alternative approach to using LiDAR remote sensing data to predict stem diameter distributions across a temperate forest landscape. Remote Sens (Basel) 9, 944. https://doi.org/10.3390/RS9090944, 2017Page 944 9.

Tamimi, R., Toth, C., 2024. Accuracy assessment of UAV LiDAR compared to traditional total station for geospatial data collection in land surveying contexts. The international archives of the photogrammetry. Remote Sens. Spatial Inf. Sci. XLVIII-2–2024, 421–426. https://doi.org/10.5194/ISPRS-ARCHIVES-XLVIII-2-2024-421-2024.

Tatay Nieto, J., 2020. La ecología integral como respuesta a los retos globales de la sostenibilidad (ODS 7, 11, 12, 13, 14, 15). Libro: Desarrollo humano integral y Agenda 2023. Aportaciones del pensamiento social cristiano a los Objetivos de Desarrollo Sostenible, Página inicial: 247, Página final: 265.

Torresani, M., Rocchini, D., Alberti, A., Moudrý, V., Heym, M., Thouverai, E., Kacic, P., Tomelleri, E., 2023. LiDAR GEDI derived tree canopy height heterogeneity reveals patterns of biodiversity in forest ecosystems. Ecol Inform 76. https://doi.org/10.1016/j.ecoinf.2023.102082.

Torre-Tojal, L., Bastarrika, A., Boyano, A., Lopez-Guede, J.M., Graña, M., 2022. Above-ground biomass estimation from LiDAR data using random forest algorithms. J. Comput. Sci. 58, 101517. https://doi.org/10.1016/J.JOCS.2021.101517.

Tsouros, D.C., Bibi, S., Sarigiannidis, P.G., 2019. A review on UAV-based applications for precision agriculture. Information (Switzerland) 10. https://doi.org/10.3390/info10110349.

Valverde, J., Barrena, V., Guillén, R., 2019. Estimación de la biomasa aérea de Eucalyptus globulus Labill plantado en cercos vivos, distrito Huertas, Junín (Perú). Revista Forestal del Perú 34, 52–65. https://doi.org/10.21704/RFP.V34I1.1285.

Van Aardt, J.A.N., Wynne, R.H., Scrivani, J.A., 2008. Lidar-based mapping of forest volume and biomass by taxonomic group using structurally homogenous segments. Photogramm Eng Remote Sensing 74, 1033–1044. https://doi.org/10.14358/PERS.74.8.1033.

Wang, F., Jia, W., Guo, H., Zhang, X., Li, D., Li, Z., Sun, Y., 2024. Point cloud-based crown volume improves tree biomass estimation: evaluating different crown volume extraction algorithms. Comput. Electron. Agric. 225, 109288. https://doi.org/10.1016/J.COMPAG.2024.109288.

Wang, L., Zhou, X., Zhu, X., Dong, Z., Guo, W., 2016. Estimation of biomass in wheat using random forest regression algorithm and remote sensing data. Crop J 4, 212–219. https://doi.org/10.1016/J.CJ.2016.01.008.

Wu, H., Xu, H., 2023. A review of sampling and modeling techniques for forest biomass inventory. Agric. Rural Studies 1. https://doi.org/10.59978/AR01010002, 0002–0002.

Yin, D., Wang, L., Lu, Y., Shi, C., 2024. Mangrove tree height growth monitoring from multi-temporal UAV-LiDAR. Remote Sens. Environ. 303, 114002. https://doi.org/10.1016/J.RSE.2024.114002.

Zamudio-Sánchez, F.J., Alvarado-Segura, A.A., De la, Cruz-De la, Cruz, K.I., Aguilar-Ávila, M., 2023. Procedimiento basado en análisis troncales para estimar a posteriori si el rendimiento maderable de un bosque ha sido sostenido a largo plazo. Revista Chapingo Serie Ciencias Forestales y del Ambiente 29, 3–24. https://doi.org/10.5154/R.RCHSCFA.2021.10.062.

Zhang, W., Qi, J., Wan, P., Wang, H., Xie, D., Wang, X., Yan, G., 2016. An easy-to-use airborne LiDAR data filtering method based on cloth simulation. Remote Sens (Basel) 8, 501. https://doi.org/10.3390/RS8060501, 2016Page 501 8.

Zhang, Y., Ma, J., Liang, S., Li, X., Li, M., 2020. An evaluation of eight machine learning regression algorithms for forest aboveground biomass estimation from multiple satellite data products. Remote Sens (Basel) 12, 4015. https://doi.org/10.3390/RS12244015, 2020Page 4015 12.

Zhen, Z., Cao, L., Liu, T., Wu, Z., Yao, F., Zhang, J., Liu, H., 2024. Estimating forest aboveground biomass using a combination of geographical random forest and empirical bayesian kriging models. Remote Sens (Basel) 16, 1859. https://doi.org/10.3390/RS16111859, 2024Page 1859 16.

Zheng, C., Abd-Elrahman, A., Whitaker, V., Dalid, C., 2022. Prediction of strawberry dry biomass from UAV multispectral imagery using multiple machine learning methods. Remote Sens (Basel) 14, 4511. https://doi.org/10.3390/RS14184511/S1.

Zhou, X., Li, C., 2023. Mapping the vertical forest structure in a large subtropical region using airborne LiDAR data. Ecol. Indic. 154, 110731. https://doi.org/10.1016/J.ECOLIND.2023.110731.

Zhu, Y., Feng, Z., Lu, J., Liu, J., 2020. Estimation of forest biomass in beijing (china) using multisource remote sensing and forest inventory data. Forests 11, 163. https://doi.org/10.3390/F11020163, 2020Page 163 11.